

# The Developmental Testbed Center WRFv3.4.1+ Surface Drag Parameterization Sensitivity Test Plan

Points of Contact: Hongli Jiang, Michelle Harrold and Jamie Wolff

November 28, 2012

## 1. Introduction

It is widely acknowledged that the Weather Research and Forecasting (WRF) model has a high surface wind speed bias, especially over plains and valleys. In recent versions of WRF, two new surface drag parameterization schemes, both associated with the Yonsei University (YSU) planetary boundary layer (PBL) scheme, have been developed. The Developmental Testbed Center (DTC) will be performing testing and evaluation of three WRF model configurations with the Advanced Research WRF (ARW) core (Skamarock et al. 2008). The baseline configuration will be run with the physics suite being used in the ARW High-Resolution Window (HIRESW) forecast system being run operationally at the National Centers for Environmental Prediction (NCEP). The two comparative configurations will be testing the effects of the surface drag parameterization scheme namelist option, *topo\_wind*, which aims to correct the high wind bias seen in WRF. One configuration will be run with *topo\_wind=1* (TWIND1; Jimenez and Dudhia 2011), which is based on the concept of a momentum sink term and makes use of the standard deviation of the subgrid-scale orography as well as the Laplacian of the topographic field. The second configuration will be run with *topo\_wind=2* (TWIND2; Mass and Ovens 2012), which determines the subgrid terrain variance and makes the surface drag or roughness used in the model dependent on it; it also includes additional consideration for stability and wind speed. The baseline configuration will have *topo\_wind=0* (turned off). These runs will be cold start cases initialized every 36 hours and run out to 48 hours for one full year.

## 2. Goals

The overarching goal of the WRFv3.4.1+ Surface Drag Parameterization Sensitivity Test is to document any changes in forecast skill between the forecasts produced by three configurations, which are exactly the same with exception to the surface drag parameterization invoked in the YSU PBL scheme using the *topo\_wind* namelist option. Forecast verification statistics will be computed for the three configurations and the analysis will be based on the objective statistics of the model output. A secondary goal of this test and evaluation will be to designate, at a minimum, the baseline configuration as a DTC Reference Configuration (RC) and widely publish the output and results for the benefit of the entire WRF community.

Additional RCs may be designated for the other two comparative configurations depending on model performance statistics.

### **3. Experiment Design**

The end-to-end forecast system will employ the WRF Preprocessing System (WPS), WRF, and Unified Post Processor (UPP). Post-processed forecasts will be verified using the Model Evaluation Tools (MET). In addition, graphics will be generated, the data will be archived and the results will be disseminated to the user community.

#### **3.1 Codes to be employed**

The baseline codes utilized will be the official released versions of WPS (v3.4.1), UPP (v2.0), and MET (v4.0). The addition of the *topo\_wind=2* option was not available in the WRF source code until the Fall of 2012, after the release of WRFv3.4.1. Thus, a tag from the WRF repository, dated 11 November 2012 (v3.4.1+) will be used for this test.

The workflow manager, Rocoto, developed by the National Oceanic and Atmospheric Administration (NOAA) Earth Systems Research Laboratory (ESRL), will be utilized to manage the execution of the end-to-end system. This workflow manager controls the system execution, starting tasks as soon as their dependencies have been met, monitoring task execution, and restarting tasks when needed.

#### **3.2 Domain Configurations**

A 15-km, and 5-km 2-way nested (*feedback=1*) domain will be employed in this test (Fig. 1). The parent domain was positioned to minimize effects of lateral boundary condition propagation into the area of interest. The inner domain was defined to limit the impacts of complex terrain at the boundaries and covers the CONUS region in order to capture complex terrain, plains and coastal regions spanning from the Gulf of Mexico, north, to Central Canada. The outer domain is 656 x 464 grid points, for a total of 304,384 grid points, while the inner domain is 1048 x 748, for a total of 783,904 grid points. The Lambert-Conformal map projection will be used and the configurations will use 36 vertical levels (37 sigma entries), with a pressure top of 50 hPa. Verification results will be computed for selected spatial aggregations, including the CONUS, CONUS-East and CONUS-West domains, along with the 14 regional sub-domains shown in Fig. 2.

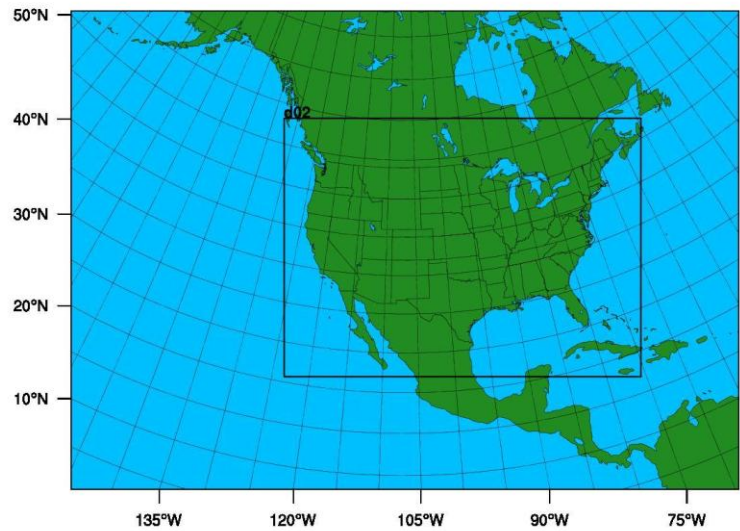


**Figure 1. Map showing the boundary of the WRF-ARW computational domain.**

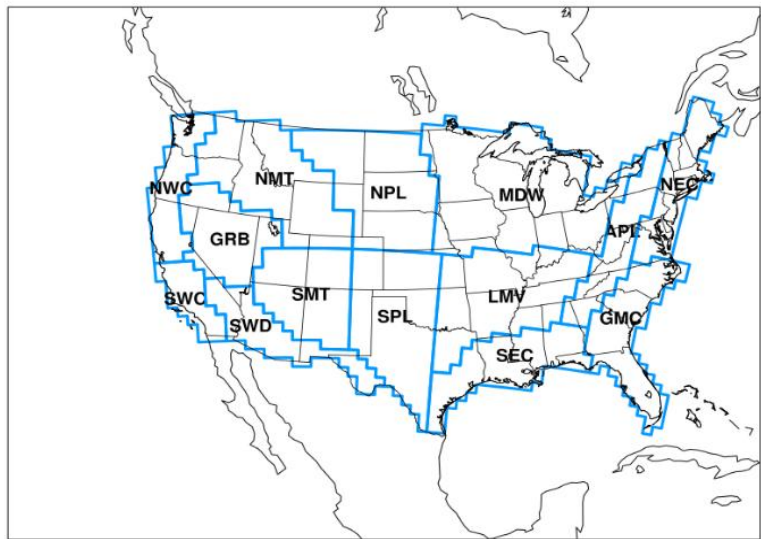


**Figure 2. Map showing the locations of the 14 regional verification domains.**

### ***3.3 Initial and Boundary Conditions***

Initial conditions (ICs) and lateral boundary conditions (LBCs) will be derived from the 0.5° x 0.5° Global Forecast System (GFS). A daily, real-time sea surface temperature product from Fleet Numerical Meteorology and Oceanography Center (FNMOC) will be used to initialize the sea surface temperature (SST) field for the forecasts. This product is produced on a near global Mercator projection with ~12 km resolution near the equator and ~9 km resolution at mid-latitudes. It is created from Advanced Very High

Resolution Radiometer (AVHRR) Global Area Coverage (GAC) satellite-retrieved SST data and in situ SST data from ships and buoys (fixed and drifting). The time-invariant component of the lower boundary conditions (topography, soil and vegetation type etc.), using United States Geological Survey (USGS) input data, will be generated through the *geogrid* program of WPS.

### 3.4 Forecast Periods

Forecasts will be initialized every 36 hours from 1 July 2011 through 30 June 2012 (Appendix B). The forecasts will be run out to 48 hours with output files generated every 3 hours. The initialization times will include 00 and 12 UTC for a total of 244 cases.

### 3.5 Physics Suites

A sample namelist is given in Appendix A. The physics suite configurations are described in Table 1 below.

**Table 1. Physics suite combinations for the surface drag parameterization sensitivity test.**

	<b>Baseline</b>	<b>TWIND1</b>	<b>TWIND2</b>
<b>Microphysics</b>	Single-Moment 3 class	Single-Moment 3 class	Single-Moment 3 class
<b>Radiation SW and LW</b>	Dudhia/RRTM	Dudhia/RRTM	Dudhia/RRTM
<b>Surface Layer</b>	Monin-Obukhov similarity theory	Monin-Obukhov similarity theory	Monin-Obukhov similarity theory
<b>Land-Surface Model</b>	Unified Noah	Unified Noah	Unified Noah
<b>PBL</b>	YSU ( <i>topo_wind=0</i> )	YSU ( <i>topo_wind=1</i> )	YSU ( <i>topo_wind=2</i> )
<b>Convection</b>	Kain-Fritsch scheme	Kain-Fritsch scheme	Kain-Fritsch scheme

### 3.6 Other Aspects of Model Configurations

A long time step of 72 s and an acoustic step of 4 s will be used. Calls to the boundary layer, and microphysics will be done every time step, whereas calls to the cumulus parameterization will be done every 5 minutes for the outer domain only; radiation will be called every 10 minutes.

The ARW solver offers a number of run-time options for the numerics, as well as various filter and damping options (Skamarock et al. 2008). The ARW will be configured to use the following numeric options: 3<sup>rd</sup>-order Runge-Kutta time integration, 5<sup>th</sup>-order horizontal momentum and scalar advection, and 3<sup>rd</sup>-order vertical momentum and scalar advection. In addition, the following filter/damping options will be utilized: three-dimensional divergence damping (coefficient 0.1), external mode filter (coefficient 0.01), off-center integration of vertical momentum and geopotential equations (coefficient 0.1), vertical-velocity damping, and a 5-km-deep diffusive damping layer at the top of the domain (coefficient 0.01). Positive-definite moisture advection will also be turned on.

### **3.7 Post-processing**

The *unipost* program within UPP will be used to destagger the forecasts, to generate derived meteorological variables, including mean sea level pressure, and to vertically interpolate fields to isobaric levels. The post-processed files will include two- and three-dimensional fields on constant pressure levels, both of which are required by the plotting and verification programs. Three-dimensional post-processed fields on model native vertical coordinates will also be made available.

### **3.8 Model Verification**

Objective model verification statistics will be generated using the MET package. MET is comprised of grid-to-point comparisons which are utilized to compare gridded surface and upper-air model data to point observations, as well as grid-to-grid comparisons which are utilized to verify quantitative precipitation forecasts (QPF).

Forecasts for surface and upper-air temperature, dewpoint, and wind will be interpolated to the location of the observations (METARs, RAOBS, and buoy data) using MET. The NCEP North American Data Assimilation System (NDAS) prepbufr files will be used as the observational dataset. Bias and bias-corrected root-mean-square-error (BCRMSE) will be computed separately for each observational type of temperature, dewpoint, and winds.

For the precipitation verification, a grid-to-grid comparison will be made in which the precipitation analyses will first be interpolated to the 15- and 5-km model integration domains and then compared to the forecast. Accumulation periods will be 3 h and 24 h. The observational datasets will be the NCEP Stage II analysis, which are available in hourly, 6-hourly and 24-hourly accumulations. The hourly data files will be summed for 3 h QPF verification and the daily data files will be used for the 24 h QPF verification. The daily accumulations are valid at 12 UTC; therefore, daily QPF will be examined for 24 and 48 h lead times for the 12 UTC initializations and 36 h lead times for the 00 UTC initializations. Traditional verification metrics computed will include the frequency bias and the Gilbert skill score.

Verification statistics will be stratified by lead time, vertical level, and regional area for 00 UTC and 12 UTC initialization hours combined. For the surface fields, forecasts will also be stratified by initialization hour (00 and 12 UTC). The regional areas for aggregation of statistics for the surface and upper-air fields will include the CONUS, CONUS-East, CONUS-West and 14 regional sub-domains (shown in Fig. 2).

Since every forecast will be run for all three configurations of the model, the presentation of the results will take advantage of the pair-wise nature of the test. With this methodology, differences between the verification statistics at individual initializations and lead times for two configurations at a time will be computed. Two sets of pair-wise difference comparisons will be made; one will evaluate REF – TWIND1, while the other will evaluate REF – TWIND2.

For surface and upper-air, both the individual and pair-wise verification statistics will be accompanied by confidence intervals (CIs) computed from standard error estimates using a correction for autocorrelation. The CIs will be computed on the median values of the stratified results for the surface and upper-air statistics using parametric tests. For the precipitation statistics, a bootstrapping method will be used. The CIs on the pair-wise differences between statistics for two configurations will assist in determining whether the differences are statistically significant.

### **3.9 Graphics Generation and Display**

Graphics will be generated using NCAR Command Language (NCL).

The suite of images generated for the REF, TWIND1 and TWIND2 configurations, and the differences between the REF – TWIND1 and REF – TWIND2 configurations will be comprised of:

- 2-m temperature with 10-m wind vectors
- 2-m dewpoint temperature with 10-m wind vectors
- 10-m wind speed and vectors
- 3-h accumulated total precipitation with MSLP and 1000-500 hPa thickness
- precipitation type
- simulated radar composite reflectivity
- snow water equivalent
- convective available potential energy
- convective inhibition
- precipitable water
- 850 hPa temperature with geopotential height and wind vectors
- 850 hPa wind speed with geopotential height and vectors
- 850 hPa relative humidity

- 850-500 hPa mean relative humidity and 700 hPa wind vectors
- 700 hPa vertical velocity with geopotential height
- 500 hPa absolute vorticity with geopotential height
- 250 hPa wind vectors with geopotential height

Finally, Skew-T soundings showing both configurations side-by-side from 14 stations (one from each sub-domain) will be created for the following sites:

- Quillayute, WA
- Vandenberg AFB, CA
- Desert Rock, NV
- Spokane, WA
- Denver, CO
- Tucson, AZ
- Rapid City, SD
- Amarillo, TX
- Davenport, IA
- Springfield, MO
- Jackson, MS
- Blacksburg, VA
- Albany, NY
- Charleston, SC

### ***3.10 Data Archival and Dissemination of Results***

Input and output data files from several stages of the end-to-end system will be archived to the NCAR High Performance Storage System (HPSS) and the results will be summarized in a report.

## ***4. Computer Resources***

- Processing resources:  
All forecasts and calculations will be computed on the NCAR supercomputer
- Storage resources:  
All archival will be done on the NCAR HPSS
- Web resources:  
Model forecast and verification graphics will be accessible through a web interface available on the DTC website

## 5. Deliverables

The NCAR HPSS will be used to archive the files produced by the forecast system. The following files will be stored:

- GFS, and SST files used for initial and boundary conditions
- Datasets used for forecast verification (NDAS Prepbufr and Stage II and NCEP/CPC precipitation analyses)
- Static files produced by the **geogrid** component of WPS
- Final output of WPS
- Input and boundary condition files produced by **real**
- History files produced by WRF
- Output of the **unipost** component of the UPP
- Output of MET
- Images produced by NCL

Additionally, all source codes and executables used will be stored. These files will be made available to the DTC and to the user community for further studies.

The DTC will produce a report outlining the results and conclusions from this test.

## 6. References

Jimenez, P. A., and J. Dudhia, 2011: Improving the Representation of Resolved and Unresolved Topographic Effects on Surface Wind in the WRF Model. *J. Appl Meteor. and Climo*, **51**, 300-315.

Mass, C. 2012: Improved Subgrid Drag of Hyper PBL/Vertical Resolution? Dealing with the Stable PBL Problems in WRF. *WRF Users' Workshop*, Boulder, CO. [Available online at:<http://www.mmm.ucar.edu/wrf/users/workshops/WS2012/ppts/3.4.pdf>]

Skamarock, W. C., J. B. Klemp, J. Dudhia, D. O. Gill, D. M. Barker, W. Wang and J. G. Powers, 2008: A Description of the Advanced Research WRF Version 3, NCAR Tech Note, NCAR/TN-475+STR, 113 pp.

### Appendix A: Subset of WRF *namelist.input* for REF

```
&time_control
run_hours           = 48,
interval_seconds    = 10800,
history_interval    = 180,
frames_per_outfile  = 1,
restart             = .false.,
io_form_history     = 2,
/
```



```

&domains
time_step                = 90,
time_step_fract_num      = 0,
time_step_fract_den      = 1,
max_dom                  = 2,
e_we                     = 656, 1048,
e_sn                     = 464, 748,
e_vert                   = 36, 36,
num_metgrid_levels      = 27,
dx                       = 15000, 5000,
dy                       = 15000, 5000,
p_top_requested          = 5000,
interp_type              = 1,
lowest_lvl_from_sfc     = .false.,
lagrange_order           = 1,
force_sfc_in_vinterp    = 1,
zap_close_levels        = 1000,
adjust_heights          = .false.,
eta_levels               = 1.000, 0.994, 0.982, 0.968, 0.950, 0.930, 0.908, 0.882, 0.853,
                        0.821, 0.788, 0.752, 0.715, 0.677, 0.637, 0.597, 0.557, 0.517,
                        0.477, 0.438, 0.401, 0.365, 0.330, 0.298, 0.268, 0.240, 0.214,
                        0.188, 0.162, 0.137, 0.114, 0.091, 0.068, 0.045, 0.022, 0.000

```

/

```

&physics
mp_physics               = 3, 3,
ra_lw_physics            = 1, 1,
ra_sw_physics            = 1, 1,
radt                     = 10, 10,
sf_sfclay_physics       = 1, 1,
sf_surface_physics      = 2, 2,
bl_pbl_physics          = 1, 1,
topo_wind                = 0, 0,
bldt                     = 0, 0,
cu_physics               = 1, 0,
cudt                     = 5,
surface_input_source     = 1,
num_soil_layers          = 4,
mp_zero_out              = 2,

```

/

```

&dynamics
diff_6th_opt          = 0, 0,
diff_6th_factor       = 0.12, 0.12,
w_damping                = 1,
diff_opt                 = 1,

```

```

km_opt           = 4,
damp_opt        = 0,
zdamp           = 5000., 5000.,
base_temp       = 290.,
dampcoef        = 0.01, 0.01,
khdif           = 0, 0,
kvdif           = 0, 0,
non_hydrostatic = .true., .true.,
scalar_adv_opt  = 1, 1,
moist_adv_opt   = 1, 1,
/

```

```

&bdy_control
spec_bdy_width  = 5,
spec_zone       = 1,
relax_zone      = 4,
specified       = .true., .false.,
nested         = .false., .true.,
/

```

## Appendix B: Case list

00 UTC Initialization	12 UTC Initialization
July 2011: 1, 4, 7, 10, 13, 16, 19, 22, 25, 28, 31	July 2011: 2, 5, 8, 11, 14, 17, 20, 23, 26, 29
August 2011: 3, 6, 9, 12, 15, 18, 21, 24, 27, 31	August 2011: 1, 4, 7, 10, 13, 16, 19, 22, 25, 28, 31
September 2011: 2, 5, 8, 11, 14, 17, 20, 23, 26, 29	September 2011: 3, 6, 9, 12, 15, 18, 21, 24, 27, 30
October 2011: 2, 5, 8, 11, 14, 17, 20, 23, 26, 29	October 2011: 3, 6, 9, 12, 15, 18, 21, 24, 27, 30
November 2011: 1, 4, 7, 10, 13, 16, 19, 22, 25, 28	November 2011: 2, 5, 8, 11, 14, 17, 20, 23, 26, 29
December 2011: 1, 4, 7, 10, 13, 16, 19, 22, 25, 28, 31	December 2011: 2, 5, 8, 11, 14, 17, 20, 23, 26, 29
January 2012: 3, 6, 9, 12, 15, 18, 21, 24, 27, 30	January 2012: 1, 4, 7, 10, 13, 16, 19, 22, 25, 28, 31
February 2012: 2, 5, 8, 11, 14, 17, 20, 23, 26, 29	February 2012: 3, 6, 9, 12, 15, 18, 21, 24, 27
March 2012: 3, 6, 9, 12, 15, 18, 21, 24, 27, 30	March 2012: 1, 4, 7, 10, 13, 16, 19, 22, 25, 28, 31
April 2012: 2, 5, 8, 11, 14, 17, 20, 23, 26, 29	April 2012: 3, 6, 9, 12, 15, 18, 21, 24, 27, 30
May 2012: 2, 5, 8, 11, 14, 17, 20, 23, 26, 29	May 2012: 3, 6, 9, 12, 15, 18, 21, 24, 27, 30
June 2012: 1, 4, 7, 10, 13, 16, 19, 22, 25, 28	June 2012: 2, 5, 8, 11, 14, 17, 20, 23, 26, 29